REGULAR ARTICLE

Polymer Journal

Vacuum-Deposited Poly(*o*-phenylenediamine)/$WO_3 \cdot nH_2O$ Nanocomposite Thin Film for NO_2 Gas Sensor

By Ashutosh TIWARI[1,†,*] *and Songjun* LI[2,†]

The vacuum-deposited thin film of hydrated tungsten oxide ($WO_3 \cdot nH_2O$) embedded poly(*o*-phenylenediamine) (PoPD/$WO_3 \cdot nH_2O$) nanocomposite was fabricated on an indium tin oxide (ITO) coated glass surface for potential NO_2 gas sensor application. The resulting PoPD/$WO_3 \cdot nH_2O$/ITO thin film was characterized using ultraviolet-visible spectroscopy (UV-vis), Fourier transform infrared spectroscopy (FT-IR), X-ray diffractometry (XRD), and electron microscopy (SEM). The composite thin film exhibited a crystalline surface morphology containing nanocrystalls of $WO_3 \cdot nH_2O$ with a diameter ranging from 5 to 10 nm. The PoPD/$WO_3 \cdot nH_2O$/ITO film allowed for the low potential detection of NO_2 gas at concentration range from 0 to 1800 ppm. The NO_2 gas sensing characteristics were studied by measuring change in the current with respect to concentration and time. The current of the PoPD/$WO_3 \cdot nH_2O$/ITO film was linearly increased with an increase in concentration of NO_2 gas with a response of ~9 s.

KEY WORDS: Poly(*o*-phenylenediamine) / Hydrated Tungsten Oxide / Vacuum-Deposition / Thin Film / Nanocomposite / NO_2 Gas Sensor /

NO_2 gas is a common air pollutant and its detection from the combustion environment is an obvious requirement. The gas sensors based on metal oxides are widely used for the detection of gases.[1–3] Among them, tungsten oxide (WO_3) is one of the most attractive technological materials for gas sensors because of its distinctive electrochromic and catalytic properties.[4–7] Recently, different types of potentiometric and amperometric gas sensors have been developed using WO_3 in the various forms such as sintered block, thick film and thin film as sensing probes.[6–9] However, these sensors could provide precise data only in a limited concentration range. Also, they are expensive, large in size, and cannot operate at room temperature. With the advent of nanotechnology, nanostructured materials with novel characteristics provide new opportunities to address these challenges.

Gas sensors based on nanostructured materials have attracted much attention because of their increased sensitivity due to the high surface-to-volume ratios.[10] Recent development of polymer-metal nanocomposites, with every imaginable combination of physical and chemical characteristics, has led to the fabrication of efficient gas sensors that can be used for a wide range of sensor applications.[11,12] Polymer nanocomposites are easy to prepare and possess high sensing efficiency with a long shelf-life. Therefore in this work, we explore a novel material based on poly(*o*-phenylenediamine) (PoPD/$WO_3 \cdot nH_2O$) nanocomposite for NO_2 gas sensor application.

Poly(*o*-phenylenediamine), PoPD is a polyaniline derivative which can be realized *via* substitution of an amino group in an aniline nucleus. The oxidative polymer of *o*-phenylenediamine has apparently shown different characteristics of molecular structure and properties in comparison with polyaniline. It is widely used as electrochemical reduction catalyst, anticorrosion coating agent, sensors, etc.[13,14] Poly(*o*-phenylenediamine) is a resinous polymer with amine (-NH_2) groups, which can be chosen as the orientation directing matrix for $WO_3 \cdot nH_2O$ because of large quantities of amino groups on the PoPD units, which have a strong binding ability to inorganic materials.[15] Moreover, in acidic condition, PoPD showed a cationic nature that may provide a template core environment to prepare quantum size composite materials. Nanosize WO_3 has gained considerable attention due to size-dependent electrical, chemical, and optical properties.[16] Thus, it should be interesting to synthesize PoPD/hydrated tungsten oxide ($WO_3 \cdot nH_2O$) nanocomposite with employing cationic polymer PoPD.

In this study, the successful attempts have been made towards the fabrication of an efficient NO_2 gas sensor based on vacuum-deposited PoPD/$WO_3 \cdot nH_2O$ nanocomposite thin film. The benefits of this technology contain self-assembly, nanoparticles, and high surface-to-volume ratio of sensing probe. The advantageous features of the present NO_2 gas sensor include low-cost, high selectivity, wide range of detection limit, and also sensor responses within ~9 s.

EXPERIMENTAL

Materials

o-Phenylenediamine (Alfa Aesar, 98%), sodium tungstate (Aldrich, 99.9%) and ammonium persulphate (Sigma, 99%) were used without further purification. All supplementary chemicals were of analytical grades. Indium-tin-oxide (ITO)

[1]Division of Engineering Materials, National Physical Laboratory, Dr. K. S. Krishnan Marg, New Delhi 110012, India
[2]Key Laboratory of Pesticide & Chemical Biology of Ministry of Education, College of Chemistry, Central China Normal University, Wuhan 430079, China
[†]Present Address: Department of Mechanical Engineering, University of Wisconsin-Milwaukee, Milwaukee-53211, Wisconsin, USA
[*]To whom correspondence should be addressed (Tel: (+91) 11-32507819, Fax: (+91) 11-25726938, E-mail: tiwaria@mail.nplindia.org, and ashunpl@gmail.com (A. Tiwari) and Lsjchem@yahoo.com.cn (S. Li)).

 doi:10.1295/polymj.PJ2009059

coated Balzers glass sheets of resistance 15 Ω/cm were used as substrates for the vacuum deposition of nanocomposite materials. The NO_2 gas standards were prepared by mixing two parts of NO gas (Zhuo Zheng gas limited company, 99.9%) with one part of oxygen (De-Luxe, 99%) in the gas bottles.[17] The gas bottles were held for two weeks to allow any residual oxygen to react with the blended NO.

Synthesis of PoPD

PoPD was prepared by the polymerization reaction of *o*-phenylenediamine using ammonium persulphate as initiator in the 5N HCl. *o*-Phenylenediamine (3 g, 0.278 moles) was mixed with 100 mL of 5N HCl under continuous stirring at 25 °C. Then, the *o*-phenylenediamine-HCl solution was taken into a three necked flask and the required amount of ammonium persulphate (0.5 g, 0.0219 moles) was continuously added drop wise to it over a period of 30 min. The resulting solution was further stirred for another 4 h. Then, the obtained orange yellow product was washed with 5N HCl. Finally, the product was dried under vacuum.

Synthesis of PoPD/$WO_3 \cdot nH_2O$ Nanocomposite

PoPD/$WO_3 \cdot nH_2O$ nanocomposite was prepared *via in situ* polymerization of *o*-phenylenediamine in the presence of 5N HCl and sodium tungstate. *o*-Phenylenediamine (3 g, 0.278 moles) was mixed with 100 mL of 5N HCl under continuous stirring at 25 °C. Then, the ammonium persulphate (0.5 g, 0.0219 moles) was added drop wise to *o*-phenylenediamine-HCl solution over a period of 30 min. Next, 10 wt % of sodium tungstate was mixed in the above solution and was further stirred for 4 h at 25 °C. Then, the obtained dark yellow product was washed with 5N HCl. Finally, the product PoPD/$WO_3 \cdot nH_2O$ nanocomposite was dried under vacuum.

Fabrication of Vacuum-Deposited PoPD/$WO_3 \cdot nH_2O$ Composite Thin Film

A rectangular pressed pallet with 12 mm diameter and 1.5 mm thickness of PoPD/$WO_3 \cdot nH_2O$ nanocomposite was prepared using hydraulic pressure machine at 6 tons/cm^2 pressure. The pellet was used as a source of PoPD/$WO_3 \cdot nH_2O$ for the preparation of thin film using vacuum thermal evaporation method at $\sim 10^{-5}$ torr pressure on the ITO coated glass substrates. Before making films, all the substrates were cleaned by successive washing with distilled water, trichloroethylene, and methanol under ultrasonic condition. The films were deposited under isothermal conditions and their thickness was measured using quartz thickness monitor.

Characterization

The adsorption spectra were recorded using an UV-visible spectrophotometer (Model 160 A, Shimadzu). FT-IR spectra were collected on a Perkin-Elmer (Spectrum BX II) spectrometer. X-Ray diffractogram was taken by Rigaku Rotaflex, RAD/Max-B, Rigaku Corporation, Japan instrument with a scanning speed of 1°/min. The surface morphology of the PoPD/ITO and PoPD/$WO_3 \cdot nH_2O$/ITO films was examined using a LEO-440 scanning electron microscope (SEM) operated at 10 kV. The films were sputter-coated with a thin layer of gold (~20 nm) prior to the morphological examination.

Detection of NO_2 Gas

The sensors were placed in a sealed Plexiglas chamber of 60 cm^3 volume. Argon was used as the carrier gas throughout the work. For humidity sensing, argon was bubbled through a bottle containing water and then mixed with dry argon. Electrical contacts were made to the sensors by connecting two short platinum wires to the electrodes using silver paste. The NO_2 gas was injected in the sensing chamber by an automatic gas-tight syringe. The total flow rate was constant at 1000 sccm, and the partial pressures of the test gases controlled with a mass flow controller. During the gas sensing study, NO_2 gas of desirable concentration was simultaneously supplied and unused NO_2 gas was taken out from chamber as exhaust gas. The changes in the current of PoPD/$WO_3 \cdot nH_2O$/ITO thin films on the exposure of NO_2 gas with respect to concentration and time were measured using a Keithley 2700 source meter having 181 nano-voltammeter and 195A digital multi-meter. The current passed through the PoPD/$WO_3 \cdot nH_2O$ thin film probes was quantitatively measured as electrical conductivity with respect to the varying concentration of NO_2 gas ranging from 0 to 1800 ppm at 0.35 V. All experiments were conducted at room temperature (~25 °C), with the same sensor used for each set of measurements. Prior to each measurement the sensors were heated in vacuum at 100 °C for 1 h to remove the chemisorbed molecules.

RESULTS AND DISCUSSION

Synthesis of PoPD and PoPD/$WO_3 \cdot nH_2O$ Nanocomposite

The PoPD was synthesized by oxidative polymerization of *o*-phenylenediamine using ammonium persulphate as oxidizing agent.[18] The ammonium persulphate was added drop-wise because the oxidation of *o*-phenylenediamine by ammonium persulphate is very sensitive to the reaction conditions. Oxidative polymerization of *o*-phenylenediamine occurs at the amine groups then a ladder PoPD polymer should be obtained. The oxidation reported here was done using $(NH_4)_2S_2O_8$ in the acidic condition, typically as the oxidation of aniline to polyaniline.[19] For the polymer synthesis, a substoichiometric amount of oxidant was used. For the polymerization a sufficient amount of oxidizing agent was used to potentially allow a ladder PoPD polymer yielding. The reaction scheme for the synthesis of PoPD is shown in Figure 1A. During the polymerization reaction, the first drop of persulphate reacts with *o*-phenylenediamine-hydrochloride to give the intermediate products.

Thereafter, the formed intermediates react with excess *o*-phenylenediamine-hydrochloride in the reaction mixture to obtain PoPD. In the other hand, hydrolysis of Na_2WO_4 in HCl is known to be complex, giving different products or intermediates depending on the pH of the reaction medium.[20] In general, Na_2WO_4 hydrolyses to form $WO_3 \cdot nH_2O$. There-

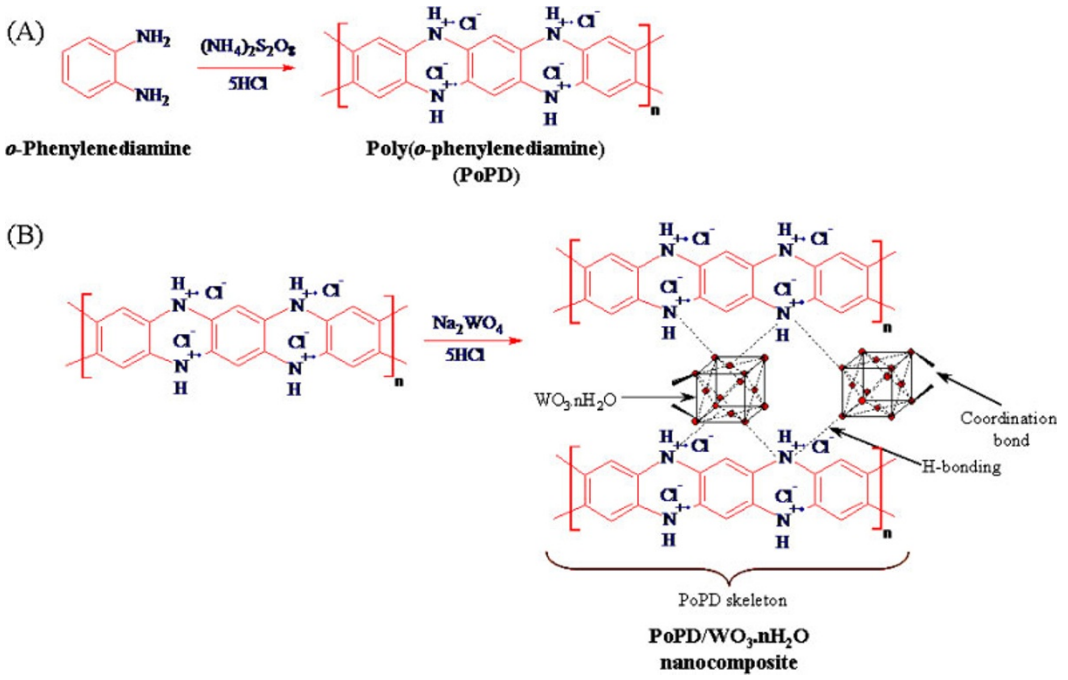

Figure 1. Synthesis of the (A) PoPD and (B) PoPD/$WO_3 \cdot nH_2O$ nanocomposite.

fore, during the preparation of PoPD/$WO_3 \cdot nH_2O$ nanocomposite, $WO_3 \cdot nH_2O$ was formed, when blending the Na_2WO_4 with PoPD in presence of HCl. In the nanocomposite, $WO_3 \cdot nH_2O$ will probably be embedded in the PoPD matrix through metal coordination and the hydrogen bonding as shown in Figure 1B.

CHARACTERIZATION

UV-visible Spectroscopy

UV-visible absorption spectra of PoPD and PoPD/$WO_3 \cdot nH_2O$ nanocomposite film is shown in Figure 2. In the spectra of PoPD (Figure 2A), an absorption peaks at about 259 was observed due to the π-π^* transition in benzeneoid ring which relates to the extent of conjugation between adjacent phenyl rings in the polymeric chain.

Moreover, a broad absorption band at 474 nm in PoPD was found due to the polarone state.[21] In the spectra of PoPD/$WO_3 \cdot nH_2O$ nanocomposite (Figure 2B), a strong absorption peak at 278 nm was observed due to nanocrystalline WO_3. A broad absorption peak appeared in the region of 461 to 490 nm is due to the polarone state in the nanocomposite. Furthermore, the absorption peak at 258 nm becomes sharp in nanocomposite thin film. This observation may be due to the orientation and interaction of $WO_3 \cdot nH_2O$ nanoparticles with PoPD.

FT-IR Spectroscopy

FT-IR spectrum of PoPD and PoPD/$WO_3 \cdot nH_2O$ nanocomposite is shown in Figure 3. In the spectrum of PoPD (Figure 3A), the bands at 3336 and 3288 cm^{-1} are due to the characteristic N-H stretching vibrations of the -NH- group at

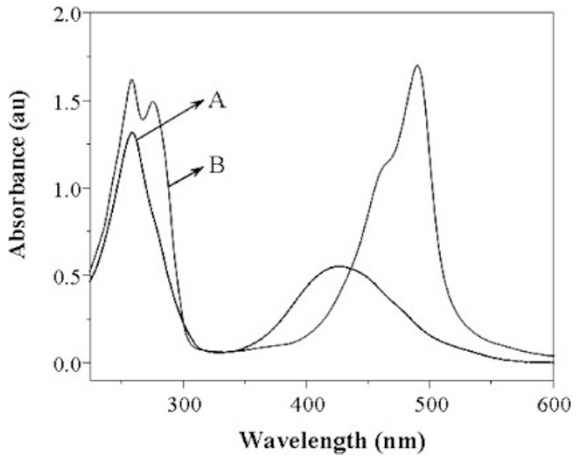

Figure 2. UV-visible absorption spectra of the (A) PoPD and (B) PoPD/$WO_3 \cdot nH_2O$ nanocomposite thin films.

two different plan. The broad peak at around 3178 cm^{-1} can be assigned to the N-H stretching vibration of the -NH_2 group.

The two bands at around 1535 and 1659 cm^{-1} are assigned to the stretching vibration of the C=C and C=N in the phenazine ring, respectively. The presence of the bands appearing at 752 and 608 cm^{-1} is characteristic of the C-H out-of-plane bending vibrations of benzene nuclei in the phenazine skeleton. The peaks at 1230 and 1362 cm^{-1} are associated with the C-N stretching in the benzenoid and quinoid imine units, respectively.[22] Whereas, in the spectrum of PoPD/$WO_3 \cdot nH_2O$ nanocomposite (Figure 3B), the absorption bands at 929, 852 and 806 cm^{-1} was observed in addition

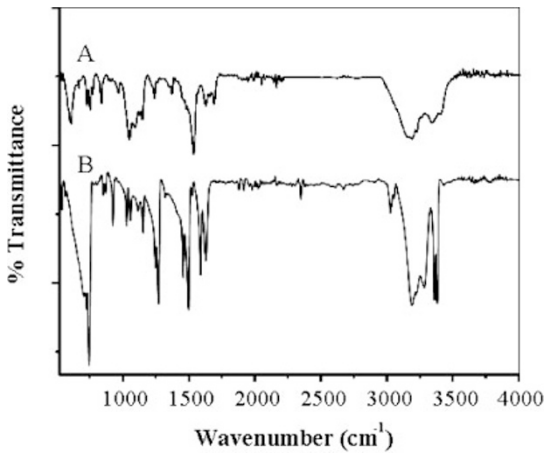

Figure 3. FT-IR spectra of the (A) PoPD and (B) PoPD/$WO_3 \cdot nH_2O$ nanocomposite thin films.

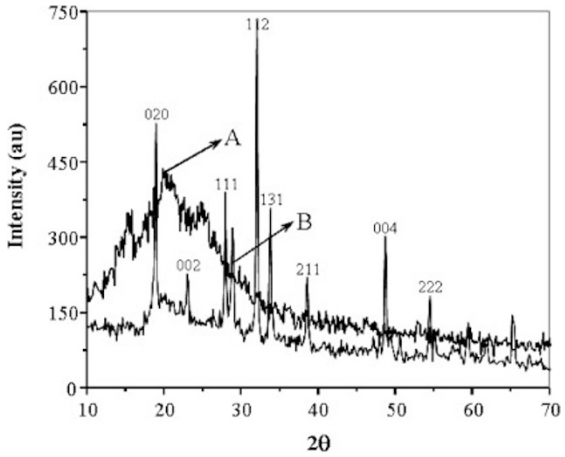

Figure 4. XRD spectra of the (A) PoPD and (B) PoPD/$WO_3 \cdot nH_2O$ nanocomposite thin films.

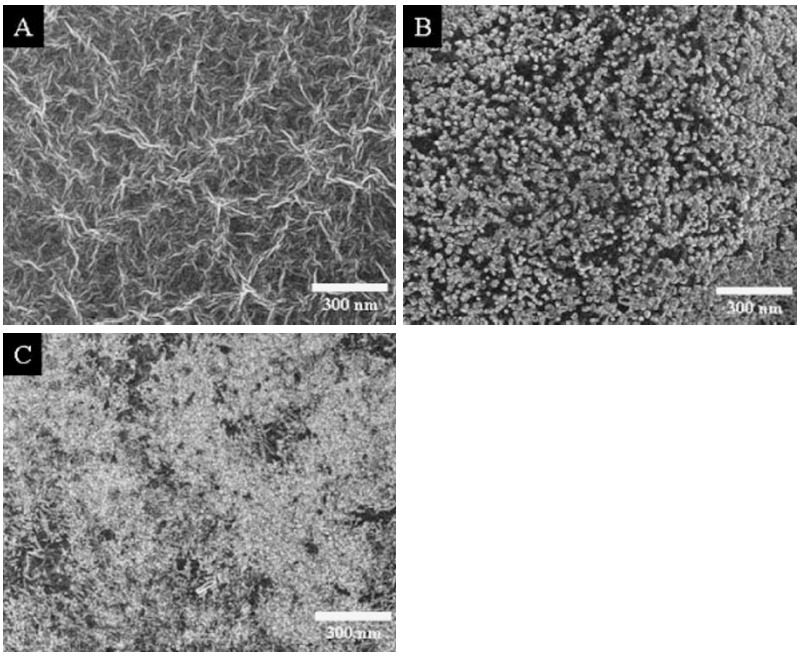

Figure 5. SEM image of the (A) PoPD, (B) drop casted PoPD/$WO_3 \cdot nH_2O$ nanocomposite, and (C) vacuum deposited PoPD/$WO_3 \cdot nH_2O$ nanocomposite thin films.

to the characteristic bands of PoPD. The bands at 929 cm^{-1} and 852 cm^{-1} are assigned to W-O stretching and at 806 cm^{-1} is due to W-O bending between tungsten and terminal oxygen. This observation clearly showed that formation of PoPD/$WO_3 \cdot nH_2O$ nanocomposite.

X-Ray Diffraction

Figure 4 shows the XRD pattern of PoPD and PoPD/$WO_3 \cdot nH_2O$ nanocomposite thin film. In the XRD pattern of PoPD (Figure 4A), the broad hump at $2\theta = 20^\circ$ suggests the amorphous nature of the PoPD polymer.

However, XRD pattern of PoPD/$WO_3 \cdot nH_2O$ nanocomposite thin film (Figure 4B) shows the sharp reflection at $2\theta = 19$ (020), 23 (002), 28 (111), 32 (112), 34 (131), 39 (211), 48 (004), and 54° (222). These peaks correspond to hydrated $WO_3 \cdot nH_2O$ nanoparticles that are present in the PoPD/$WO_3 \cdot nH_2O$ nanocomposite. The crystallite size of $WO_3 \cdot nH_2O$ inside the PoPD/$WO_3 \cdot nH_2O$ nanocomposite was calculated using the Scherrer equation[23] and was found to be in the range of ~8 nm.

SEM Study

The surface morphology of the PoPD, drop casted PoPD/$WO_3 \cdot nH_2O$, and vacuum deposited PoPD/$WO_3 \cdot nH_2O$ nanocomposite thin films was examined by SEM. As shown in Figure 5A, the PoPD thin film was found to be porous weaved surface. The SEM image of drop casted PoPD/$WO_3 \cdot nH_2O$ nanocomposite thin film (Figure 5B) shows the formation of rough microstructure having uniformly distributed cubic crystalline $WO_3 \cdot nH_2O$ nanoparticles in the polymer.

It was observed that the cubic sphere of $WO_3 \cdot nH_2O$ nanoparticles (crystallite size ~35–50 nm) consisted of a solid cubic shell that allowed polymer matrix out of the cubic structure. However, microstructure of vacuum deposited PoPD/$WO_3 \cdot nH_2O$ nanocomposite thin film (Figure 5C) illustrates a homogeneous distribution of tiny crystalline $WO_3 \cdot nH_2O$ nanoparticles in the porous PoPD polymer matrix. The estimated value of crystallite size was found to be about 5–10 nm, which is probably due to the formation of clusters of $WO_3 \cdot nH_2O$ nanoparticles in the thin film. In this context, the vacuum deposited PoPD/$WO_3 \cdot nH_2O$ nanocomposite film has a unique surface structure and can provide a high surface-to-volume ratio to NO_2 gas adsorption over the thin film, while drop casted PoPD/$WO_3 \cdot nH_2O$ nanocomposite film has comparatively poor capability for the same. Moreover, during the vacuum deposition of the PoPD/$WO_3 \cdot nH_2O$ nanocomposite film, the incorporation of $WO_3 \cdot nH_2O$ nanoparticles into the PoPD polymeric network introduces porosity that may create the diffusion channels inside the polymeric networks. The uniformly distributed $WO_3 \cdot nH_2O$ nanoparticles along with the porosity in PoPD matrix are expected to be advantageous for gas sensor.

Gas Sensing Behavior

The NO_2 gas sensing behaviors of vacuum deposited PoPD/ITO and PoPD/$WO_3 \cdot nH_2O$ nanocomposite films were evaluated by the reported method.[24] The change in the current of the sensing probes (*c.f.*, PoPD/ITO and PoPD/$WO_3 \cdot nH_2O$/ITO) as a function of time and NO_2 concentration was recorded at room temperature. The sensitivities of the sensors were estimated from the measured value of current in air and in presence of NO_2 gas. The graphs of changes in current of the PoPD/ITO and PoPD/$WO_3 \cdot nH_2O$/ITO probes as a function of time are shown in Figure 6.

With exposure of NO_2 gas (1200 ppm) to probes, the sudden increase in current was observed in the both case. The PoPD/ITO film has response time of ~30 s but recovery time was almost double *i.e.*, about 22 s to PoPD/$WO_3 \cdot nH_2O$/ITO probe (Figure 6A). This observation may be due to the unique surface structure and electronic behavior of the vacuum deposited PoPD/$WO_3 \cdot nH_2O$ nanocomposite film, can have ability to provide a high surface-to-volume ratio to NO_2 gas adsorption in a limited time period. Moreover, easy recovery of the vacuum deposition of the PoPD/$WO_3 \cdot nH_2O$ nanocomposite sensor (Figure 6B) was responsible due the incorporation of $WO_3 \cdot nH_2O$ nanoparticles into the PoPD polymeric network that introduced the porosity which probably created the good diffusion channels to NO_2 gas inside the PoPD polymer/$WO_3 \cdot nH_2O$ nanocomposite networks. The uniformly distributed $WO_3 \cdot nH_2O$ nanoparticles along with the porous PoPD matrix are expected to be a sharp and specific NO_2 gas sensing response.

Moreover, the original current was achieved, when the NO_2 gas had been turned off and fresh air was introduced into the test chamber. The insert of fresh air in the test chamber remove the adsorb gas molecules from the probe surface and regain the original current. The observed changes in the current of both the probes (*i.e.*, PoPD/ITO and PoPD/$WO_3 \cdot nH_2O$/ITO) are due to physical adsorption of NO_2 gas on the surface of respective films.

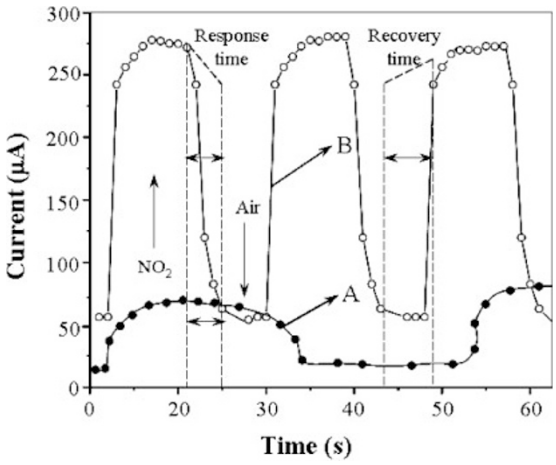

Figure 6. The current response of the (A) PoPD/ITO and (B) PoPD/$WO_3 \cdot nH_2O$/ITO nanocomposite probes, with respect to time ranging from 0 to 63 s on the exposure of 1200 ppm NO_2 gas at 0.35 V.

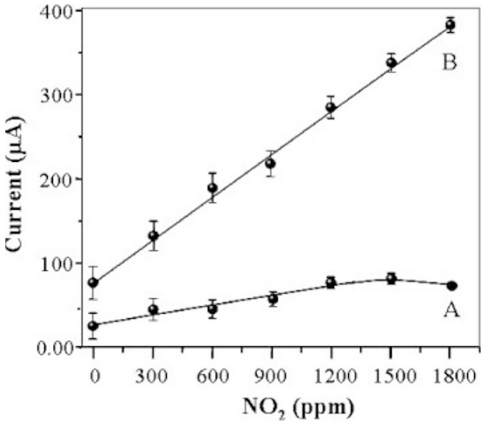

Figure 7. The current response of the (A) PoPD/ITO and (B) PoPD/$WO_3 \cdot nH_2O$/ITO nanocomposite probes on the exposure of 0 to 1800 ppm NO_2 gas at 0.35 V.

Figure 7 shows the variation of current versus NO_2 gas concentration profile of PoPD/ITO and PoPD/$WO_3 \cdot nH_2O$/ITO probes. The current increases with an increase in NO_2 gas concentration ranging from 0 to 1800 ppm in case of PoPD/$WO_3 \cdot nH_2O$/ITO probe but PoPD/ITO probe showed linearity with NO_2 gas concentration ranging from 0 to 1500 ppm. In general, the interaction of NO_2 gas with the π-electron network of PoPD capture the electron from the polymer and decrease the resistance of probe from 0 to 1500 ppm of NO_2 gas (Figure 7A). While, $WO_3 \cdot nH_2O$ is an n-type semiconductor; they will create a more space charge region at the $WO_3 \cdot nH_2O$-PoPD interface in the case of the PoPD/$WO_3 \cdot nH_2O$/ITO probe. During NO_2 gas adsorption, a high conductivity and sensing range of sensing probe was achieved in the PoPD/$WO_3 \cdot nH_2O$/ITO probe due to reduction of space charge region

in the PoPD/$WO_3 \cdot nH_2O$ nanocomposite matrix (Figure 7B). The modulation of space charge region at the interface of $WO_3 \cdot nH_2O$-PoPD gives a high range of sensitivity for NO_2 gas and hence PoPD/$WO_3 \cdot nH_2O$/ITO probe can operate at room temperature. Also, in this study, a relatively fast response (~9 s) and recovery (~10 s) time was observed for NO_2 gas using PoPD/$WO_3 \cdot nH_2O$/ITO sensor. The observed fast response time of PoPD/$WO_3 \cdot nH_2O$ thin film to NO_2 gas is well below, when compared to the other NO_2 gas sensors reported in the literature.[25–28]

Sensing Mechanism

In earlier studies, NO_2 was reported to have large effects on the conductivity of polymer films.[29,30] It is interpreted that a charge transfer complex is formed between the PoPD/$WO_3 \cdot nH_2O$ film donor and NO_2 acceptor, and the charge carriers are the holes produced in the polymeric matrix. NO_2 is π-electron acceptor, and accepted electron would delocalize over the NO_2 planar structure. The high selectivity towards the NO_2 gas may be explained on the basis of charge transfer complex formed between the PoPD/$WO_3 \cdot nH_2O$ film donor and NO_2 gas acceptor molecules to cause fluctuation in terms of current.[31,32] These studies supported that the PoPD/$WO_3 \cdot nH_2O$ nanocomposite thin film has ability to sense NO_2 gas specifically.

Interference and Storage Stability

The effect of interferents (NH_3, NO and CO_2) was studied on the current responses of the PoPD/$WO_3 \cdot nH_2O$/ITO probe (Table I). These three substances were added into the gas sensing chamber at their normal physical concentration, *i.e.*, NH_3 (500 ppm); NO (500 ppm); and CO_2 (1000 ppm).

It was found that the presence of interferents had a negligible effects on the current response obtained; therefore, using this probe, NO_2 can be detected without any interference. Table II compares the characteristics of conducting polymer based NO_2 gas sensors as reported in the literature. From this table it is clearly observed that PoPD/$WO_3 \cdot nH_2O$/ITO probe exhibited a longer shelf life, higher selectivity, and shorter response time in a wider range.

The lifetime of the PoPD/$WO_3 \cdot nH_2O$/ITO probe was determined by measuring the current up to ~5 months at an interval of seven days. It was observed that the current decreased slowly with the increase in time period. After 5 months, the decrease in current was found to be about 32%.

Table I. Effect of interference on the PoPD/$WO_3 \cdot nH_2O$/ITO NO_2 gas sensor at 0.35 V

Sl. No.	Analyte/Interference	Current (mA)
1.	NO_2 (1200 ppm)	278
2.	NO_2 (1200 ppm) + NH_3 (500 ppm)	286
3.	NO_2 (1200 ppm) + NO (500 ppm)	282
4.	NO_2 (1200 ppm) + CO_2 (1000 ppm)	272

Table II. Comparison between different materials tested for the NO_2 gas sensors

Sensing probe	Linearity with [NO_2], ppm	Response time, Seconds	Shelf-life, Months	Reference
PoPD/$WO_3 \cdot nH_2O$ nanocomposite thin film	0–1800	~9	~5	Present work
PANI/polystyrenesulfonic acid composite film	20–100	10	—	22
PANI-SnO_2 composite film	10–800	1000	—	12
PANI nanofibers	10–200	100	~4	23
Au-doped WO_3	5–20	500	~3	24
Mesoporous WO_3 thin films	3–100	60–120	—	25
Scandia-stabilised zirconia (8 mol % Sc_2O_3-ZrO_2) solid electrolyte and CuO + $CuCr_2O_4$ mixed-oxide	10–500	8	—	26

CONCLUSIONS

PoPD/$WO_3 \cdot nH_2O$ nanocomposite was synthesized by self assembled *in situ* polymerization reaction. PoPD/$WO_3 \cdot nH_2O$ nanocomposite thin film was successfully fabricated on ITO coated glass substrate using vacuum deposition method as efficient sensors for detection of NO_2 gas. The PoPD/$WO_3 \cdot nH_2O$/ITO probe can be operated at room temperature for sensing NO_2 gas in the wide concentration rage. This is an added advantage of PoPD/$WO_3 \cdot nH_2O$ nanocomposite thin film when compared to other types of sensors reported for sensing NO_2 gas. The response time and recovery time of PoPD/$WO_3 \cdot nH_2O$ sensor was found to be ~9 s and ~10 s, respectively, which shows that the PoPD/$WO_3 \cdot nH_2O$ sensor could be reused more frequently that extends the shelf life of the sensor.

Acknowledgment. Authors are thankful to the Department of Science and Technology, Govt. of India and to the National Science Foundation of China (Grant No. 20603010) for generous financial supports and to the Director, National Physical Laboratory, New Delhi, India for providing infrastructure facilities to carry out this work.

Received: March 13, 2009
Accepted: May 25, 2009
Published: July 9, 2009

REFERENCES

1. E. Comini, *Anal. Chim. Acta*, **568**, 28 (2006).
2. O. K. Tan, W. Cao, Y. Hu, and W. Zhu, *Ceram. Int.*, **30**, 1127 (2004).
3. O. K. Tan, W. Caob, Y. Hua, and W. Zhu, *Solid State Ionics*, **172**, 309 (2004).
4. X. Wang, N. Miura, and N. Yamazoe, *Sens. Actuators, B*, **66**, 74 (2000).
5. C. J. Jin, T. Yamazaki, Y. Shirai, T. Yoshizawa, T. Kikuta, N. Nakatani, and H. Takeda, *Thin Solid Films*, **474**, 255 (2005).
6. J. L. Solis, S. Saukko, L. B. Kish, C. G. Graqvist, and V. Lantto, *Sens. Actuators, B*, **77**, 316 (2001).
7. I. Jimenez, J. Arbiol, G. Dezanneau, A. Cornet, and J. R. Morante, *Sens. Actuators, B*, **93**, 475 (2003).

8. M. Stankova, X. Vilanova, E. Llobet, J. Calderer, M. Vinaixa, I. Gracia, C. Canec, and X. Correig, *Thin Solid Films*, **500**, 302 (2006).
9. K. Galatsis, X. X. Li, W. Wlodarski, and K. Kalantar-Zadel, *Sens. Actuators, B*, **87**, 478 (2001).
10. A. Tiwari and S. Gong, *Electroanalysis*, **20**, 1775 (2008).
11. M. K. Ram, O. Yavuz, V. Lahsangahand, and M. Aldissi, *Sens. Actuators, B*, **156**, 750 (2005).
12. M. K. Ram, O. Yavuz, and M. Aldissi, *Synth. Met.*, **151**, 77 (2005).
13. T. Ohsaka, T. Watanabe, F. Kitamura, N. Oyama, and K. Tokuda, *Chem. Commun.*, **16**, 1072 (1991).
14. C. Malitesta, F. Palmisano, L. Torsi, and P. G. Zambonin, *Anal. Chem.*, **62**, 2735 (1990).
15. P. A. Kumar, M. Ray, and S. Chakraborty, *J. Hazard. Mater.*, **143**, 24 (2007).
16. W. Morales, M. Cason, O. Aina, N. R. deTacconi, and K. Rajeshwar, *J. Am. Chem. Soc.*, **130**, 6318 (2008).
17. S. Vaughan, *Gases & Instrumentation*, **1**, 26 (2007).
18. J. Han, G. Song, and R. Guo, *Eur. Polym. J.*, **43**, 4229 (2007).
19. A. Tiwari and V. Singh, *Carbohydr. Polym.*, **74**, 427 (2008).
20. E. F. Sperenskaya, V. E. Mertsalova, and I. I. Kulev, *Russ. Chem. Rev.*, **35**, 892 (1966).
21. A. Tiwari, V. Sen, S. R. Dhakate, A. P. Mishra, and V. Singh, *Polym. Adv. Technol.*, **19**, 909 (2008).
22. A. Tiwari, *J. Macromol. Sci., Part A: Pure Appl. Chem.*, **44**, 735 (2007).
23. H. P. Klug and L. E. Alexander, in "X-Ray Diffraction Procedures for Polycrystalline and Amorphous Materials," 2nd ed., Wiley Inter-Science, 1974, Chap. 9.
24. D. Xie, Y. Jiang, W. Pan, D. Li, Z. Wu, and Y. Li, *Sens. Actuators, B*, **81**, 158 (2002).
25. X. B. Yan, Z. J. Hana, Y. Yanga, and B. K. Taya, *Sens. Actuators, B*, **123**, 107 (2007).
26. H. Xia, Y. Wang, F. Kong, S. Wang, B. Zhu, X. Guo, J. Zhang, Y. Wang, and S. Wu, *Sens. Actuators, B*, **134**, 133 (2008).
27. L. G. Teoh, Y. M. Hon, J. Shieh, W. H. Lai, and M. H. Hon, *Sens. Actuators, B*, **96**, 219 (2003).
28. W. Xiong and G. M. Kale, *Sens. Actuators, B*, **114**, 101 (2006).
29. R. L. van Ewyk, A. V. Chadwick, and J. D. Wright, *J. Chem. Soc., Faraday Trans I*, **76**, 2194 (1980).
30. S. Radhakrishnan and S. G. Joshi, *J. Polym. Sci., Part C: Polym. Lett.*, **27**, 127 (1989).
31. A. Tiwari, *J. Polym. Res.*, **15**, 337 (2008).
32. T. G. J. V. Oirschot, D. V. Leeuwen, and J. Medema, *J. Electroanal. Chem.*, **37**, 373 (1972).

